Measurement of the mixing state of PAHs in individual particles and its effect on PAH transport in urban and remote areas and from major sources

Xiufeng Lian [a,b,c], Guohua Zhang [b,d], Yuxiang Yang [b], Mubai Chen [a,c], Wenda Yang [a,c], Chunlei Cheng [a,c], Bo Huang [e], Zhong Fu [e], Xinhui Bi [b,d], Zhen Zhou [a,c], Mei Li [a,c,*]

[a] Institute of Mass Spectrometry and Atmospheric Environment, Guangdong Provincial Engineering Research Center for On-line Source Apportionment System of Air Pollution, Jinan University, Guangzhou, 510632, PR China
[b] State Key Laboratory of Organic Geochemistry and Guangdong Provincial Key Laboratory of Environmental Protection and Resources Utilization, Guangzhou Institute of Geochemistry, Chinese Academy of Sciences, Guangzhou, 510640, PR China
[c] Guangdong-Hongkong-Macau Joint Laboratory of Collaborative Innovation for Environmental Quality, Guangzhou, 510632, PR China
[d] Guangdong-Hong Kong-Macao Joint Laboratory for Environmental Pollution and Control, Guangzhou Institute of Geochemistry, Chinese Academy of Sciences, Guangzhou, 510640, PR China
[e] Guangzhou Hexin Analytical Instrument Company Limited, Guangzhou, 510530, China

ARTICLE INFO

ABSTRACT

Although recent laboratory simulations have demonstrated that organic matter prevents the degradation of polycyclic aromatic hydrocarbons (PAHs), their role in the long-range transport of PAHs in the real atmosphere remains poorly understood. In this study, we measured the chemical composition and mixing state of PAHs-containing individual particles in aerosols from three sources, one urban area and one remote area. PAHs-containing particles were classified into five types: organic carbon (OC), potassium mixed with organic carbon (KOC), potassium mixed with sodium (KNa), Krich and PAH-rich. The PAH-rich and KOC particles were the main types of particles produced by vehicle exhaust/coal burning and biomass burning, respectively, accounting for >50% of the PAHs-containing particles. It was found that organic matter enhancement of PAHs-containing particles occurs in the ambient atmosphere, with organic-rich (OC and KOC) particles accounting for >90%. Further analysis revealed that the increase in the fractions of PAHs was related to the mixing state with organic compounds due to the protection of organics against PAHs and/or the aging of PAHs-containing particles. The results of this study improve our understanding of the chemical composition and mixing state of PAHs particles in atmospheric aerosols from emission sources and urban and remote areas, and provide field observation evidence to support the promotion of the study of long-range transport of PAHs by organics.

Credit author statement

Xiufeng Lian: Methodology and Writing-original draft. **Guohua Zhang:** Writing-original draft. **Yuxiang Yang:** Sampling. **Mubai Chen:** Sampling. **Wenda Yang:** Sampling. **Chunlei Cheng:** Writing-original draft. **Bo Huang:** Sampling. **Zhong Fu:** Writing-original draft. **Xinhui Bi:** Writing-original draft. **Zhen Zhou:** Writing-original draft. **Mei Li:** Methodology and Writing-original draft.

1. Introduction

Over the past two decades, polycyclic aromatic hydrocarbons (PAHs) have received widespread attention owing to their carcinogenic and mutagenic effects on ecosystems and humans (Dat and Chang, 2017; Hsu et al., 2019; Li et al., 2019; Ma et al., 2020; Pratt et al., 2018; Shrivastava et al., 2017; Yan et al., 2019). Although the concentration of PAHs has decreased significantly under relevant policies (Dat and Chang, 2017; Liao and Yu, 2020; Zhan et al., 2022), the measured concentrations of PAHs in recent years have still been higher than the acceptable threshold recommended by the World Health Organization (WHO) (Boström et al., 2002). Numerous studies have focused on the concentrations (Kim et al., 2013; Wang et al., 2011), sources (Yang et al., 2010), emission factors (Eiguren-Fernandez and Miguel, 2012), environmental and human health effects (Hsu et al., 2019; Ma et al., 2020), and gas-particle

partitioning coefficients (Ma et al., 2019; Pratt et al., 2018), and have simulated long-range transport processes (Galarneau et al., 2014; Lohmann and Lammel, 2004). Presently, our unclear understanding of the long-range transport mechanism of PAHs is a key issue impeding our understanding of the fate of PAHs and in reducing model uncertainty.

PAHs are released from both natural and anthropogenic sources (Cai et al., 2018; Ishtiaq et al., 2021; Lammel and Gerhard, 2015; Li et al., 2016a; Lin et al., 2015). Natural sources of PAHs include forest and grassland fires, volcanic eruptions, and plant and microorganism biosynthesis (Itoh et al., 2017; Wang et al., 2017). Anthropogenic sources include vehicle exhaust, biomass burning, coal burning, and industrial sources (Li et al., 2016b; Mu et al., 2014; Wei et al., 2015; Yao et al., 2020; Zhang et al., 2011). Biomass burning, domestic coal burning, vehicle and industrial emissions are the main sources of PAHs emissions in China, contributing much more than in other countries, and these sources emit a higher proportion of PAHs with carcinogenic potential (Liao and Yu, 2020; Wang et al., 2019; Yan et al., 2019; Youping and Xin, 2015).

Once discharged into the atmosphere, PAHs are redistributed in the gaseous and particulate phases, which affects their deposition, degradation, and transport (Dat and Chang, 2017; Liu et al., 2015; Ma et al., 2013; Wu et al., 2017; Zhu et al., 2022). During transportation, PAHs react with atmospheric oxidants (ozone, hydroxyl radicals, and nitrogen oxide) or undergo photolysis forming PAHs derivatives (oxy-PAHs, nitro-PAHs, etc.) (Bandowe and Meusel, 2017; Lara et al., 2022; Lin et al., 2015; Tomaz et al., 2016), or are removed from the atmosphere via dry and/or wet deposition (Lv et al., 2016; Ma et al., 2013; Zeng et al., 2021). Gas-phase PAHs usually have shorter atmospheric lifetimes than those found on particulates due to the faster oxidation or photolysis rates (Vione et al., 2004). Laboratory measurements have shown that PAHs adsorbed onto the surfaces of elemental carbon, solid organic carbon, and ammonium sulfate particles react quickly with ozone or NO_3 radicals, and their atmospheric lifetimes range from several minutes to a few hours (Liu et al., 2012; Zhou et al., 2013). Even so, high concentrations of PAHs have been detected in the Arctic surface seawater and boundary-layer air (Ma et al., 2013; Yu et al., 2019).

Despite decades of research, the mechanisms responsible for the long-range transport of PAHs were not completely clear. This is mainly due to our incomplete understanding of the gas-particle partitioning and chemical loss rates of PAHs (Lammel and Gerhard, 2015; Shimada et al., 2020). Previous laboratory studies have shown that secondary organic aerosol (SOA) coatings can effectively protect PAHs from ozone (Berkemeier et al., 2016; Pankow, 1994; Shiraiwa et al., 2017; Zhou et al., 2013). The degradation rates of PAHs and SOA coatings in the real atmosphere depends on the characteristics of emission sources and regional changes (Shimada et al., 2020; Shrivastava et al., 2017). The temperature and humidity conditions in different regions affect the phase states of the organic aerosols and further affect the degradation of PAHs (Mu et al., 2018; Shiraiwa et al., 2017). Model results have shown that in warm/humid environments, aerosol particles tend to be liquid, while in cold environments, aerosols are semi-solid or solid (Shiraiwa et al., 2017). In addition, the phase state of the SOA coating depends on the chemical composition of the SOA coating (Mu et al., 2018; Shiraiwa et al., 2013). Liquid organic coatings do not significantly shield PAHs from ozone (Zhou et al., 2012, 2013). Compared with the traditional absorption-adsorption partitioning of PAHs on black carbon and organic aerosol models (Lohmann and Lammel, 2004; Sehili and Lammel, 2007; Wang et al., 2011), the model shields PAHs from heterogeneous oxidation, greatly reducing the negatively modified normalized mean bias (Shrivastava et al., 2017). Although the concentration analysis results of three sampling sites at different distance along the same transmission trajectory provide evidence for the protective effect of SOA coatings on PAHs (Shimada et al., 2020), the traditional membrane sampling technology does not observe the mixing state of PAHs and SOAs, which affects the mechanism by which organic aerosols effect the long-range transmission of PAHs in the actual environment.

To clarify how the chemical compositions of in atmospheric aerosols affect the long-range transport of PAHs, a single-particle mass spectrum (SPMS) was used to observe the PAHs-containing particles in the aerosols from biomass burning, vehicle exhaust, biomass burning, and ambient aerosols from Guangzhou and Mt. Tianjing in southern China. We investigated the chemical composition and mixing state of the PAHs-containing particles, and analyzed the effect of the chemical composition on the long-range transport of PAHs. Our results help clarify the long-range transport mechanism of PAHs and provide a scientific basis for improving the model.

2. Methodology

2.1. Sampling

Ambient aerosol particles were measured from January 1 to January 18, 2020, at the Jinan University (JNU) atmospheric supersite (23°7′ 48″ N, 113°21′ E; 35 m a.s.l.), and from November 13 to December 8, 2020 at the Mt. Tianjing site (24°41′ 56″ N, 112°53′ 56″ E; 1690 m a.s.l.) in southern China. The Guangzhou urban site was located at the top of the library building, which was surrounded by teaching and residential areas, representing a typical urban environment in the Pearl River Delta region (Sun et al., 2020). The remote site was surrounded by a forest park (273 km²) and was unaffected by anthropogenic activities (Lin et al., 2017). Samples were collected using an online single-particle aerosol mass spectrometer (SPAMS) through a $PM_{2.5}$ cyclone sampling inlet.

The aerosol particles from the emission sources were directly collected using a vacuum flask connected to a smoke gun, and then imported into a SPAMS for analysis (see Supporting Information (**SI**)). Table 1 shows the number of PAHs-containing and the total number of all the detected particles. The meteorological data, including temperature, relative humidity (RH), wind speed, and wind direction data, as well as $PM_{2.5}$ and gaseous pollutants, were simultaneously determined.

2.2. Instrumentation

The individual particle sizes and chemical compositions were analyzed by a SPAMS (Hexin Analytical Instrument Co., Ltd., Guangzhou, China). More details of the SPAMS analysis method have been described elsewhere (Li et al., 2011); therefore, we only brief describe the method here. The aerosol particles were drawn through a 0.1-mm orifice and focused into a narrow beam in the aerodynamic focusing lens. Subsequently, they were aerodynamically sized using two continuous diode Nd:YAG laser beams (532 nm). Then a pulsed laser (266 nm) desorbed and ionized the chemical components of each particle based on the flight time during sizing. The positive and negative ions generated from the particles were detected using a dual-polar time-of-flight spectrometer.

2.3. Data analysis

All of the single particle data were imported into MATLAB and analyzed using the FATEs toolkit (Shingler et al., 2012). The PAHs-containing particles were detected by the presence of *m/z* 152

Table 1
Summary of SPAMS measurements and numbers of all the detected particles and PAHs-containing particles.

	Source/Site	All detected particles	PAHs
Sources	Coal burning	8834	8149
	Biomass burning	6086	1699
	Vehicle exhaust	6631	4537
Urban	Guangzhou	4 461 595	27 717
Remote	Mt. Tianjing	990 891	4766

$[C_{12}H_{10}]^+$ (acenaphthylene), 178 $[C_{14}H_{10}]^+$ (anthracene or phenanthrene), 165 $[C_{13}H_9]^+$ (acenaphthylene), (pyrene or fluoranthene), 202 $[C_{14}H_{10}]^+$ (pyrene or fluoranthene), 226 $[C_{18}H_{10}]^+$/228 $[C_{18}H_{12}]^+$ (chrysene or benzo [a]anthracene), and 252 $[C_{20}H_{12}]^+$ (benzo [b]fluoranthene or benzo [k]fluoranthene or benzo [a]pyrene) (Bente et al., 2009; Silva and Prather, 2000; Wilson et al., 2013). Additionally, mixed sources refer to all of the PAHs-containing particles produced by coal burning, vehicle exhaust, and biomass burning.

Overall, 8 149, 4 537, and 1699 particles in the 0.2–2.0 μm size range (d_{va}) were identified as PAHs-containing particles, resulting from coal burning, vehicle exhaust, and biomass burning, respectively. A total of 27 717 and 4766 particles were identified as PAHs-containing particles at the Guangzhou, and Mt. Tianjing sites, accounting for 0.62% and 0.48% of the total detected particles, respectively. These PAHs-containing particles were clustered using the adaptive resonance algorithm (ART-2a) method based on the similarities of mass-to-charge ions and peak intensities (Song et al., 1999). The parameters for the ART-2a analysis were a vigilance factor of 0.8, a learning rate of 0.05, and interactions at 20. Based on the characteristics of the ion peaks and peak intensities in the positive spectra of the PAHs-containing particles, five particle types with distinct mass spectra characteristics were identified for further analyses. As is shown in Fig. S1, the mass spectral patterns of the potassium mixed with organic carbon (KOC) showed a strong K^+ (m/z 39 $[K^+]$), a series of weak organic carbon (OC) fragments (m/z 27 $[C_2H_3]^+$, 29 $[C_2H_5]^+$, 37 $[C_3H]^+$, 51 $[C_4H_3]^+$, and 63 $[C_5H_3]^+$). A high abundance of m/z 39 in the mass spectra of the KOC may be due to the coagulation of OC and $[K]^+$ or the condensation of organic species onto biomass or industrial seed particles (Moffet et al., 2008). The OC particles were characterized in a series of OC fragments with K^+. The Krich type was characterized by the highest peak at m/z 39 $[K]^+$, are presumably derived from biomass and/or biofuel burning (Bi et al., 2011). The potassium mixed with sodium (KNa) particles had the highest peak at m/z 39 $[K]^+$ and a smaller peak at m/z 23 $[Na]^+$. The KNa type particles are believed to be formed from industrial emissions, sea salt, and/or dry lake beds (Moffet et al., 2008). The PAH-rich type exhibited strong m/z 152 $[C_{12}H_{10}]^+$ or 165 $[C_{13}H_9]^+$ or 178 $[C_{14}H_{10}]^+$ or 202 $[C_{16}H_{10}]^+$ or 226 $[C_{18}H_{10}]^+$ peaks in the positive spectrum.

2.4. Backward trajectories

The spatial distributions of the number fractions of PAHs-containing particles associated with the backward trajectories (72 h) of air masses at 1800 m bove the ground at Mt. Tianjing were determined. The cluster trajectories were calculated by MeteoInfo (Wang, 2014).

3. Results and discussion

3.1. Source profile of PAHs-containing particles

Fig. 1 shows the average positive and negative mass spectra of the PAHs-containing particles from vehicle exhaust, coal burning, and biomass burning. The PAHs-containing particles from vehicle exhaust contained strong m/z 43 $[C_2H_3O]^+$ and PAHs fragments (m/z 165 $[C_{13}H_9]^+$, 178 $[C_{14}H_{10}]^+$, and 202 $[C_{16}H_{10}]^+$) and weak elemental carbon (EC) ions (m/z −48 $[C_4]^-$ and−60 $[C_5]^-$), N-organic ions (m/z −26 $[CN]^-$), nitrate (m/z −46 $[NO_2]^-$ and −62 $[NO_3]^-$), and sulfate (m/z −97 $[HSO_4]^-$) peaks in the negative spectrum. The PAHs-containing particles produced by coal burning exhibited a series of weak peaks including m/z 39 $[K^+]$, OC fragments (m/z 51 $[C_4H_3]^+$ and 63 $[C_5H_3]^+$), and PAH fragments (m/z 152 $[C_{12}H_{10}]^+$, 165 $[C_{13}H_9]^+$, 178 $[C_{14}H_{10}]^+$, 202 $[C_{16}H_{10}]^+$, 226 $[C_{18}H_{10}]^+$, and 252 $[C_{20}H_{12}]^+$). The PAHs-containing particles produced by biomass burning were characterized by intense peaks at m/z 39 $[K^+]$, which were significantly higher than the abundances of K^+ in the other two sources. Weak nitrate and PAH fragments (m/z 165 $[C_{13}H_9]^+$, 178 $[C_{14}H_{10}]^+$, 202 $[C_{16}H_{10}]^+$, and 228 $[C_{18}H_{12}]^+$) were observed in the PAHs-containing particles produced by biomass
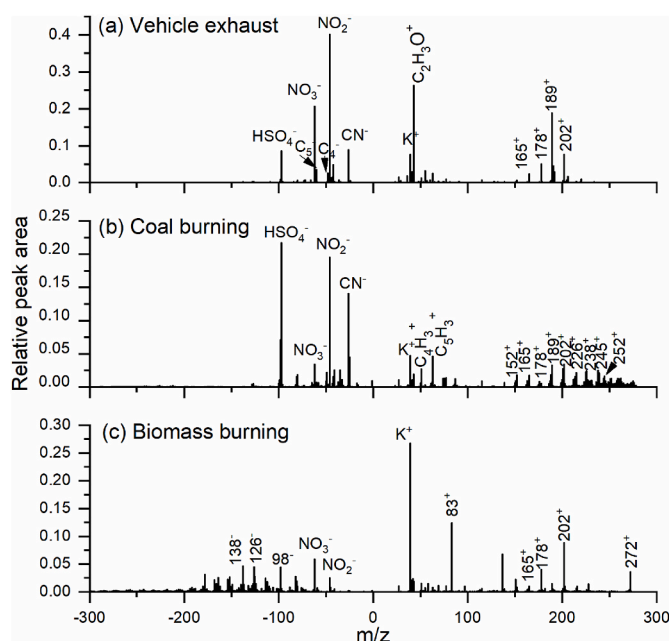

Fig. 1. Average mass spectra of PAHs-containing particles from vehicle exhaust, coal burning, and biomass burning.

burning. The relative peak area ratio of $m/z = -46$ to $m/z = -62$ was greater than 1 for the vehicle exhaust and coal burning aerosols, which may strongly indicate the presence of nitrated PAHs (NPAHs) (Fitzpatrick et al., 2008; Wilson et al., 2013; Zhang et al., 2023). More abundant m/z 226 $[C_{18}H_{10}]^+$ and 252 $[C_{20}H_{12}]^+$ were observed in PAHs-containing particles produced by coal burning, corresponding to the higher concentrations of benz [a]anthracene, benzo [a]pyrene, and benzo [b]fluoranthene in the coal burning aerosols (Dat and Chang, 2017). The average positive and negative mass spectra of the PAHs-containing particles collected at Guangzhou and Mt. Tianjing sites are shown in Fig. S2.

3.2. Comparison of PAHs-containing particles in sources and ambient aerosols

Fig. 2(a) descripts the relative number abundance distribution of the main types of PAHs-containing particles in the coal burning, vehicle exhaust, and biomass burning sources. The relative abundance of all of the types of particles in the coal burning source was similar to that in the vehicle exhaust source, but it was distinctly different from that in the biomass burning source. KOC was the main particle type in the biomass burning particles, accounting for 65.6%, while PAH-rich particles were the main type in the coal burning and vehicle exhaust particles, accounting for 60.3% and 52.6%, respectively. The OC particles were the second most important particle type among the three emission sources. There were more PAHs with molecular weights greater than 202, sulfates and nitrogenous organics in PAHs-containing particles from biomass burning than those from vehicle exhaust (Fig. S3). The PAH-rich and OC particles are the two particle types with the largest number fractions of PAHs-containing particles from the coal burning and vehicle exhaust sources, accounting for more than 98% of the total PAHs-containing particles. This is consistent with the results of Su et al. (2021) regarding the highest number fraction of PAHs mixed with organics from vehicle exhaust in the idling state. Moreover, a significant fraction (65.6%) of KOC particles was found in biomass burning aerosols, followed by OC particles (27.7%). Previous studies have shown that KOC has the highest abundance in atmospheric biomass burning particles (Bi et al., 2011), so it can be used as a characteristic of biomass burning particles to distinguish them from other emission sources (Yang
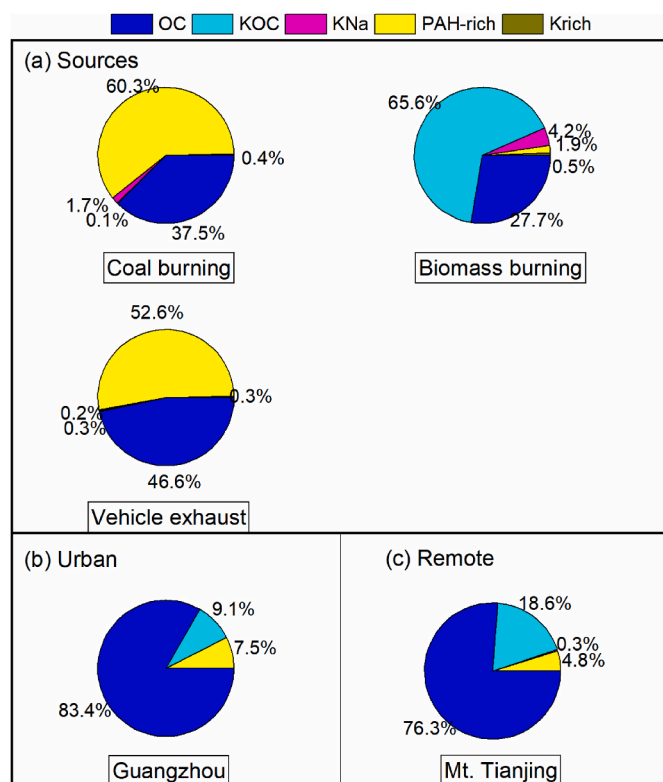
Fig. 2. Relative number abundance distributions of the main types of PAHs-containing particles in the aerosol from the emission sources (coal burning, biomass burning, and vehicle exhaust), and at the urban (Guangzhou) and remote (Mt. Tianjing) sites.

Fig. 3. Mass spectra subtraction plot of the average mass spectra corresponding to (a) Guangzhou minus mixed sources, and (b) Mt. Tianjing minus Guangzhou.

et al., 2017). Therefore, KOC is likely to be used as a reference marker for biomass burning PAHs-containing particles in ambient aerosols.

The number fractions of organics (m/z 27 $[C_2H_3]^+$ and 43 $[C_2H_3O]^+$) in the atmosphere at the Guangzhou (79%–86%) and Mt. Tianjing (83%–91%) sites were significantly higher than those in the source aerosols (17%–45% and 57%–82%, respectively; Fig. S3), and the relative peak areas of the nitrate, sulfate, and OC fragments (e.g., m/z 27 $[C_2H_3]^+$, 37 $[C_3H_3]^+$, etc.) exhibited a pronounced enhancement are the Guangzhou site relative to the sources (Fig. 3(a)). Relative peak area of the N-organic ion (m/z −26 $[CN]^-$ and −42 $[CNO]^-$) enhancement was observed at the Mt. Tianjing site compared to with the Guangzhou site (Fig. 3(b)). These organic ions may have been due to the presence of C–N bonds (Zawadowicz et al., 2017), which are the fragment peaks of complex nitrated organics such as organic nitrates, nitroaromatics, nitrogen heterocycles, and polyphenols. Furthermore, more than 90% (by number, OC and KOC) of the PAHs were internally mixed with organics at the Guangzhou and Mt. Tianjing sites, respectively (Fig. 2(b) and (c)), and the fraction of organic-poor (PAH-rich) particles are the Mt. Tianjing site sharply decreased by 36% compared with that at the Guangzhou site.

3.3. Comparison of PAH-containing particles in different air mass sources

The spatial distributions of the PAHs-containing particles associated with the backward trajectories (72 h) of the air masses at 100 m levels above the ground at Guangzhou and at 1800 m above the ground at Mt. Tianjing are shown in Fig. 4. The cluster trajectories were calculated using the MeteoInfo software (Wang, 2014). At Mt. Tianjing site, Clusters 2 and 3 started in different regions, but they both passed through similar areas in Guangxi Province. Clusters 2 originated in northeast India, and Clusters 3 originated in central Myanmar. Higher number fractions (0.61% and 0.44%) of the total PAHs-containing particles were
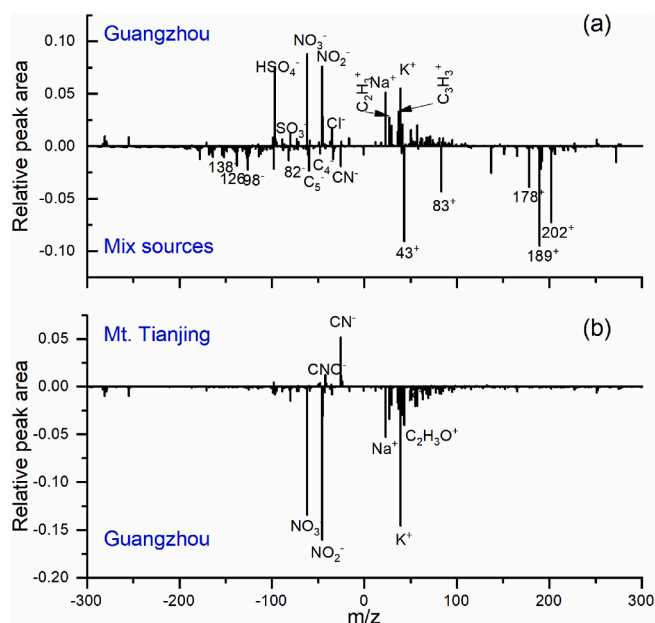
associated with the air masses of Cluster 3 (20%) and Cluster 1 (68%), from the regions to the southwest and southeast of the sampling site, respectively. The T and SO_2, NO_x, O_3 and $PM_{2.5}$ concentrations were higher during the transport of Cluster 1 than during the transport of Clusters 2 and 3. The $PM_{2.5}$ and T were higher and the wind speed was lower during the transport of Cluster 3 than during the transport Cluster 2 (Table 2). There were no significant correlations between the number fraction of the PAHs-containing particles and meteorological factors (Table S2), indicating that the number fraction of PAHs-containing particles was mainly affected by the source of the air mass. Consistent with the results presented in Section 3.2, more PAHs were internally mixed with organics in air Cluster 1 and Cluster 3. At Guangzhou site, Clusters 1 and 2 originated in Jiangxi Province and Fujian Province, respectively, and Cluster 3 originated from the East China Sea. The number fractions of PAHs-containing in Clusters 1 and 2 were higher than that in cluster 3, which is consistent with the results reported in previous studies that anthropogenic sources are the main sources of PAHs (Liao and Yu, 2020; Wang et al., 2019). In addition, the fraction of PAHs during the transport cluster 1 was 0.15% higher than that in cluster 2, and the sum of OC and KOC during the transport cluster 2 was 1%, which is lower than that in cluster 1. It may be related to the protective effect of organic compounds.

To distinguish the influences of the emission sources and particulate mixing state, the relationship between the particulate mixing state of the same air mass and the number fraction of PAHs-containing particles at Mt. Tianjing site was analyzed. In Cluster 1 and Cluster 3, for a total number of PAH particles of greater than 1000, the fraction of PAHs-containing particles was further divided into low, medium and high PAHs based on the number fractions of the PAHs-containing particles. As is shown in Fig. 5, when the fractions of organic-rich (OC and KOC) particles increased from 90% to 98%, the fraction of PAHs-containing particles increased from 0.2% to 3.0%. Moreover, the relative abundance of OC particles in Cluster 3 increased by 30% for high PAHs relative to low PAHs.

3.4. Most likely mechanism for the organic-enhanced PAHs

The experimental results revealed that the PAHs were locked in aerosols with highly viscous semi-solid secondary organic aerosols during the particle aging, which slowed down the volatilization and
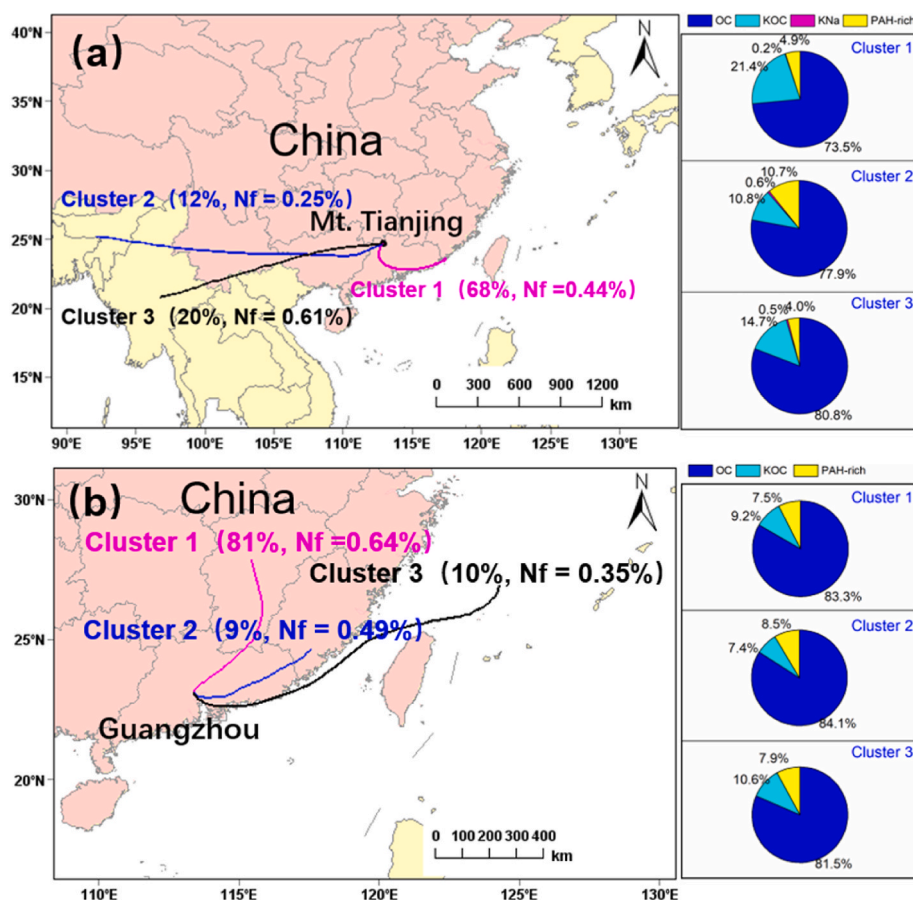
Fig. 4. Spatial distributions of the number fractions of PAHs-containing particles associated with the backward trajectories (72 h) of the air masses at 1800 m above the ground at Mt. Tianjing and at 100 m levels above the ground at Guangzhou. Relative number abundance distributions of the main types of PAHs-containing particles in the aerosols from Clusters 1, 2 and 3. Nf represents the number fractions of PAHs-containing particles in all of the measured particles in each cluster.

Table 2
The average values and standard deviations of the meteorological parameters and the concentrations of pollutants during Clusters 1, 2, and 3.

Air mass	SO$_2$	NO$_x$	O$_3$	PM$_{2.5}$	T (°C)	RH< (%)	WS< (m/s)
	(μg/m^3)						
Cluster 1	1.0 ± 1.1	3.7 ± 3.2	70 ± 19	5.0 ± 6.2	12.4 ± 2.7	90 ± 15	3.8 ± 1.7
Cluster 2	0.6 ± 0.5	3.1 ± 1.5	65 ± 14	2.6 ± 3.5	3.6 ± 3.4	94 ± 9	5.2 ± 3.1
Cluster 3	0.6 ± 0.2	3.1 ± 1.5	67 ± 11	4.5 ± 3.9	7.3 ± 5.8	88 ± 14	3.8 ± 2.5

oxidation of the PAHs (Zelenyuk et al., 2012). The model considering the shielding effect of organics reduced the negative corrected normalized mean deviations of the urban and remote areas by 43% and 54%, respectively, compared with the traditional model (Shrivastava et al., 2017). This conclusion is further supported by the shielding of PAHs by SOAs, which resulted in higher PAHs concentrations at remote locations (Shimada et al., 2020). Unfortunately, based on the available data, we could not accurately quantify the shielding effect of organic compounds on PAHs. The long-range transport is also an important factor for particle aging (Feng et al., 2015; Yuan et al., 2020; Zhang et al., 2020). The number fractions of OC-containing particles in the aerosols emitted from combustion sources and transported over long distances are an order of magnitude greater than that of aerosols emitted from local sources (Zhang et al., 2020). The long-range transport of inland air pollutants is an important contributor to the organics in the fine atmospheric
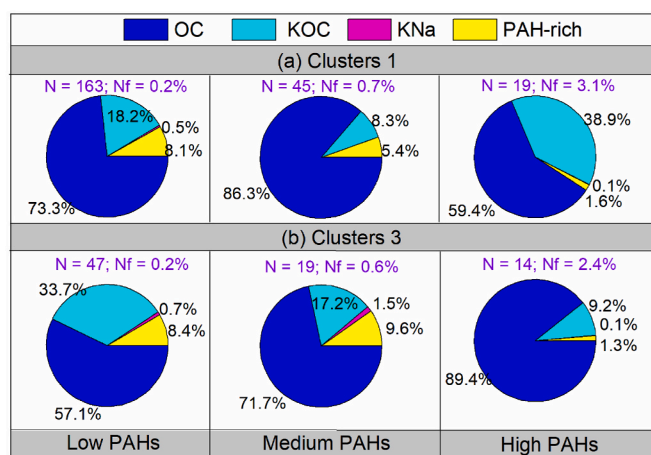

Fig. 5. Relative number abundance distributions of the main types of PAHs-containing particle as a function of the number fractions of PAHs-containing particles. N represents the duration (hours) of the sampling; and Nf represents the number fraction of the total number of PAHs-containing particles divided by the total number of particles.

particles (Yuan et al., 2020). Regional transport is one of the important sources of PAHs in urban environments (Zhang et al., 2017). In this study, the finding that increase in the fraction of PAH particles was accompanied by an increase in the organic-rich particles in different air masses and an increase in the PAH abundance (Fig. 5), supports the

hypothesis of the possible protective effect of organic compounds on PAHs. Moreover, the fact that the number fractions of the NPAHs in the particles composed of PAHs mixed with organics were approximately 20%–30% lower than that those of other types of particles in this study (Fig. S4) further supports this hypothesis.

4. Conclusions and implications

The chemical compositions and mixing state of the individual of PAHs-containing particles in ambient atmospheric particles obtained from emission sources, an urban site, and a remote site were analyzed to investigate long-range transport of PAHs in the ambient atmosphere. Our results provide observational data for the extension of laboratory results to the ambient atmosphere, and indicate that organics prevent PAHs from degrading (Zelenyuk et al., 2012), thus allowing the PAHs to travel longer distances. PAH-rich and KOC particles were the main particle types produced by vehicle exhaust/coal burning and biomass burning, respectively. The abundances of organic material in the PAH particles collected at the urban and remote sites were significantly higher than those in the PAHs from the emission sources. More than 80% of the particles in the ambient aerosols were mixed with organics, and the high fraction of PAH particles was often related to a high degree of mixing with organics. These results may be partly due to organics protecting the PAHs from oxidation and partly due to particulate aging. Previous studies have shown that elemental carbon plays an important role in PAH transport (Friedman et al., 2014). However, Fig. S5 shows that the number fraction of elemental carbon ions (36 $[C_3]^+$) was significantly higher in the PAHs-containing particles than in all of the detected particles, suggesting that elemental carbon play a weak role. Overall, our results provide insights into the mixing state of PAH-containing particles and underscore the importance of organics in the long-range transport of PAHs, which advance our understanding of PAH transport mechanisms and have far-reaching implications for improving the accuracy of PAH transport models.

Declaration of competing interest

The authors declare that they have no known competing financial interests or personal relationships that could have appeared to influence the work reported in this paper.

Data availability

Data will be made available on request.

Acknowledgments

Appendix A. Supplementary data

Supplementary data to this article can be found online at https://doi.org/10.1016/j.envres.2022.114075.

References

Bandowe, B.A.M., Meusel, H., 2017. Nitrated polycyclic aromatic hydrocarbons (nitro-PAHs) in the environment – a review. Sci. Total Environ. 581–582, 237–257.

Bente, M., Sklorz, M., Streibel, T., Zimmermann, R., 2009. Thermal Desorption−Multiphoton ionization time-of-flight mass spectrometry of individual aerosol particles: a simplified approach for online single-particle analysis of polycyclic aromatic hydrocarbons and their derivatives. Anal. Chem. 81, 2525–2536.

Berkemeier, T., Steimer, S.S., Krieger, U.K., Peter, T., Pöschl, U., Ammann, M., Shiraiwa, M., 2016. Ozone uptake on glassy, semi-solid and liquid organic matter and the role of reactive oxygen intermediates in atmospheric aerosol chemistry. Phys. Chem. Chem. Phys. 18, 12662–12674.

Bi, X., Zhang, G., Li, L., Wang, X., Li, M., Sheng, G., Fu, J., Zhou, Z., 2011. Mixing state of biomass burning particles by single particle aerosol mass spectrometer in the urban area of PRD, China. Atmos. Environ. 45, 3447–3453.

Boström, C.-E., Gerde, P., Hanberg, A., Jernström, B., Johansson, C., Kyrklund, T., Rannug, A., Törnqvist, M., Victorin, K., Westerholm, R., 2002. Cancer risk assessment, indicators, and guidelines for polycyclic aromatic hydrocarbons in the ambient air. Environ. Health Perspect. 110 (Suppl. 3), 451–488.

Cai, C., Yu, S., Li, X., Liu, Y., Tao, S., Liu, W., 2018. Emission characteristics of polycyclic aromatic hydrocarbons from pyrolytic processing during dismantling of electronic wastes. J. Hazard Mater. 351, 270–276.

Dat, N.-D., Chang, M.B., 2017. Review on characteristics of PAHs in atmosphere, anthropogenic sources and control technologies. Sci. Total Environ. 609, 682–693.

Eiguren-Fernandez, A., Miguel, A.H., 2012. Size-resolved polycyclic aromatic hydrocarbon emission factors from on-road gasoline and diesel vehicles: temperature effect on the nuclei-mode. Environ. Sci. Technol. 46, 2607–2615.

Feng, J., Hu, J., Xu, B., Hu, X., Sun, P., Han, W., Gu, Z., Yu, X., Wu, M., 2015. Characteristics and seasonal variation of organic matter in PM2.5 at a regional background site of the Yangtze River Delta Region, China. Atmos. Environ. 123, 288–297.

Fitzpatrick, E.M., Jones, J.M., Pourkashanian, M., Ross, A.B., Williams, A., Bartle, K.D., 2008. Mechanistic aspects of soot formation from the combustion of pine wood. Energy Fuel. 22, 3771–3778.

Friedman, C.L., Pierce, J.R., Selin, N.E., 2014. Assessing the influence of secondary organic versus primary carbonaceous aerosols on long-range atmospheric polycyclic aromatic hydrocarbon transport. Environ. Sci. Technol. 48, 3293–3302.

Galarneau, E., Makar, P.A., Zheng, Q., Narayan, J., Zhang, J., Moran, M.D., Bari, M.A., Pathela, S., Chen, A., Chlumsky, R., 2014. PAH concentrations simulated with the AURAMS-PAH chemical transport model over Canada and the USA. Atmos. Chem. Phys. 14, 4065–4077.

Hsu, C.-Y., Chiang, H.-C., Chen, M.-J., Yang, T.-T., Wu, Y.-S., Chen, Y.-C., 2019. Impacts of hazardous metals and PAHs in fine and coarse particles with long-range transports in Taipei City. Environ. Pollut. 250, 934–943.

Ishtiaq, J., Syed, J.H., Jadoon, W.A., Hamid, N., Iqbal Chaudhry, M.J., Shahnawaz, M., Nasir, J., Haider Rizvi, S.H., Chakraborty, P., Li, J., Zhang, G., 2021. Atmospheric polycyclic aromatic hydrocarbons (PAHs) at urban settings in Pakistan: spatial variations, sources and health risks. Chemosphere 274, 129811.

Itoh, N., Naya, T., Kanai, Y., Kumon, F., Amano, K., 2017. Historical changes in the aquatic environment and input of polycyclic aromatic hydrocarbons over 1000 years in Lake Kitaura, Japan. Limnology 18, 51–62.

Kim, K.-H., Jahan, S.A., Kabir, E., Brown, R.J.C., 2013. A review of airborne polycyclic aromatic hydrocarbons (PAHs) and their human health effects. Environ. Int. 60, 71–80.

Lammel, Gerhard, 2015. Polycyclic aromatic compounds in the atmosphere - a review identifying research needs. Polycycl. Aromat. Comp.: J. Int. Soc. Polycycl. Aromat. Comp. 35, 316–329.

Lara, S., Villanueva, F., Martín, P., Salgado, S., Moreno, A., Sánchez-Verdú, P., 2022. Investigation of PAHs, nitrated PAHs and oxygenated PAHs in PM10 urban aerosols. A comprehensive data analysis. Chemosphere 294, 133745.

Li, H., Wang, Y., Li, H., Zhu, C., Mao, H., Yang, M., Wang, R., Wang, W., 2016a. Investigation of sources of atmospheric polycyclic aromatic hydrocarbons at Mt. Lushan in southern China. J. Geophys. Res. Atmos. 121, 3050–3061.

Li, J., Li, X., Li, M., Lu, S., Yan, J., Xie, W., liu, C., Qi, Z., 2016b. Influence of air pollution control devices on the polycyclic aromatic hydrocarbon distribution in flue gas from an ultralow-emission coal-fired power plant. Energy Fuel. 30, 9572–9579.

Li, L., Huang, Z., Dong, J., Li, M., Gao, W., Nian, H., Fu, Z., Zhang, G., Bi, X., Cheng, P., 2011. Real time bipolar time-of-flight mass spectrometer for analyzing single aerosol particles. Int. J. Mass Spectrom. 303, 118–124.

Li, Y., Juhasz, A.L., Ma, L.Q., Cui, X., 2019. Inhalation bioaccessibility of PAHs in PM2.5: implications for risk assessment and toxicity prediction. Sci. Total Environ. 650, 56–64.

Liao, K., Yu, J.Z., 2020. Abundance and sources of benzo[a]pyrene and other PAHs in ambient air in Hong Kong: a review of 20-year measurements (1997–2016). Chemosphere 259, 127518.

Lin, Q., Zhang, G., Peng, L., Bi, X., Wang, X., Brechtel, F.J., Li, M., Chen, D., Peng, P., Sheng, G., Zhou, Z., 2017. In situ chemical composition measurement of individual cloud residue particles at a mountain site, southern China. Atmos. Chem. Phys. 17, 8473–8488.

Lin, Y., Ma, Y., Qiu, X., Li, R., Fang, Y., Wang, J., Zhu, Y., Hu, D., 2015. Sources, transformation, and health implications of PAHs and their nitrated, hydroxylated, and oxygenated derivatives in PM2.5 in Beijing. J. Geophys. Res. Atmos. 120, 7219–7228.

Liu, C., Zhang, P., Yang, B., Wang, Y., Shu, J., 2012. Kinetic studies of heterogeneous reactions of polycyclic aromatic hydrocarbon aerosols with NO3 radicals. Environ. Sci. Technol. 46, 7575–7580.

Liu, Y., Gao, Y., Yu, N., Zhang, C., Wang, S., Ma, L., Zhao, J., Lohmann, R., 2015. Particulate matter, gaseous and particulate polycyclic aromatic hydrocarbons

(PAHs) in an urban traffic tunnel of China: emission from on-road vehicles and gas-particle partitioning. Chemosphere 134, 52–59.

Lohmann, R., Lammel, G., 2004. Adsorptive and absorptive contributions to the gas-particle partitioning of polycyclic aromatic hydrocarbons: state of knowledge and recommended parametrization for modeling. Environ. Sci. Technol. 38, 3793–3803.

Lv, Y., Li, X., Xu, T.T., Cheng, T.T., Yang, X., Chen, J.M., Iinuma, Y., Herrmann, H., 2016. Size distributions of polycyclic aromatic hydrocarbons in urban atmosphere: sorption mechanism and source contributions to respiratory deposition. Atmos. Chem. Phys. 16, 2971–2983.

Ma, W.-L., Zhu, F.-J., Liu, L.-Y., Jia, H.-L., Yang, M., Li, Y.-F., 2019. PAHs in Chinese atmosphere: gas/particle partitioning. Sci. Total Environ. 693, 133623.

Ma, W.-L., Zhu, F.-J., Liu, L.-Y., Jia, H.-L., Yang, M., Li, Y.-F., 2020. PAHs in Chinese atmosphere Part II: health risk assessment. Ecotoxicol. Environ. Saf. 200, 110774.

Ma, Y., Xie, Z., Yang, H., Möller, A., Halsall, C., Cai, M., Sturm, R., Ebinghaus, R., 2013. Deposition of polycyclic aromatic hydrocarbons in the north pacific and the arctic. J. Geophys. Res. Atmos. 118, 5822–5829.

Moffet, R.C., de Foy, B., Molina, L.T., Molina, M.J., Prather, K.A., 2008. Measurement of ambient aerosols in northern Mexico City by single particle mass spectrometry. Atmos. Chem. Phys. 8, 4499–4516.

Mu, L., Peng, L., Liu, X., Song, C., Bai, H., Zhang, J., Hu, D., He, Q., Li, F., 2014. Characteristics of polycyclic aromatic hydrocarbons and their gas/particle partitioning from fugitive emissions in coke plants. Atmos. Environ. 83, 202–210.

Mu, Q., Shiraiwa, M., Octaviani, M., Ma, N., Ding, A., Su, H., Lammel, G., PöSchl, U., Cheng, Y., 2018. Temperature effect on phase state and reactivity controls atmospheric multiphase chemistry and transport of PAHs. Sci. Adv. 4, eaap7314.

Pankow, J.F., 1994. An absorption model of gas/particle partitioning of organic compounds in the atmosphere. Atmos. Environ. 28, 185–188.

Pratt, G.C., Herbrandson, C., Krause, M.J., Schmitt, C., Lippert, C.J., McMahon, C.R., Ellickson, K.M., 2018. Measurements of gas and particle polycyclic aromatic hydrocarbons (PAHs) in air at urban, rural and near-roadway sites. Atmos. Environ. 179, 268–278.

Sehili, A.M., Lammel, G., 2007. Global fate and distribution of polycyclic aromatic hydrocarbons emitted from Europe and Russia. Atmos. Environ. 41, 8301–8315.

Shimada, K., Nohchi, M., Yang, X., Sugiyama, T., Miura, K., Takami, A., Sato, K., Chen, X., Kato, S., Kajii, Y., Meng, F., Hatakeyama, S., 2020. Degradation of PAHs during long range transport based on simultaneous measurements at Tuoji Island, China, and at Fukue Island and Cape Hedo, Japan. Environ. Pollut. 260, 113906.

Shingler, T., Dey, S., Sorooshian, A., Brechtel, F.J., Wang, Z., Metcalf, A., Coggon, M., Mülmenstädt, J., Russell, L.M., Jonsson, H.H., Seinfeld, J.H., 2012. Characterisation and airborne deployment of a new counterflow virtual impactor inlet. Atmos. Meas. Tech. 5, 1259–1269.

Shiraiwa, M., Li, Y., Tsimpidi, A.P., Karydis, V.A., Berkemeier, T., Pandis, S.N., Lelieveld, J., Koop, T., Pöschl, U., 2017. Global distribution of particle phase state in atmospheric secondary organic aerosols. Nat. Commun. 8, 15002.

Shiraiwa, M., Zuend, A., Bertram, A.K., Seinfeld, J.H., 2013. Gas–particle partitioning of atmospheric aerosols: interplay of physical state, non-ideal mixing and morphology. Phys. Chem. Chem. Phys. 15, 11441–11453.

Shrivastava, M., Lou, S., Zelenyuk, A., Easter, R.C., Corley, R.A., Thrall, B.D., Rasch, P.J., Fast, J.D., Massey Simonich, S.L., Shen, H., Tao, S., 2017. Global long-range transport and lung cancer risk from polycyclic aromatic hydrocarbons shielded by coatings of organic aerosol. P. Natl. Acad. Sci. 114, 1246–1251.

Silva, P.J., Prather, K.A., 2000. Interpretation of mass spectra from organic compounds in aerosol time-of-flight mass spectrometry. Anal. Chem. 72, 3553–3562.

Song, X.H., Hopke, P.K., Fergenson, D.P., Prather, K.A., 1999. Classification of single particles analyzed by ATOFMS using an artificial neural network, ART-2A. Anal. Chem. 71, 860–865.

Su, B., Zhang, G., Zhuo, Z., Xie, Q., Du, X., Fu, Y., Wu, S., Huang, F., Bi, X., Li, X., Li, L., Zhou, Z., 2021. Different characteristics of individual particles from light-duty diesel vehicle at the launching and idling state by AAC-SPAMS. J. Hazard Mater. 418, 126304.

Sun, J.Y., Wu, C., Wu, D., Cheng, C., Li, M., Li, L., Deng, T., Yu, J.Z., Li, Y.J., Zhou, Q., Liang, Y., Sun, T., Song, L., Cheng, P., Yang, W., Pei, C., Chen, Y., Cen, Y., Nian, H., Zhou, Z., 2020. Amplification of black carbon light absorption induced by atmospheric aging: temporal variation at seasonal and diel scales in urban Guangzhou. Atmos. Chem. Phys. 20, 2445–2470.

Tomaz, S., Shahpoury, P., Jaffrezo, J.-L., Lammel, G., Perraudin, E., Villenave, E., Albinet, A., 2016. One-year study of polycyclic aromatic compounds at an urban site in Grenoble (France): seasonal variations, gas/particle partitioning and cancer risk estimation. Sci. Total Environ. 565, 1071–1083.

Vione, D., Barra, S., de Gennaro, G., de Rienzo, M., Gilardoni, S., Perrone, M.G., Pozzoli, L., 2004. Polycyclic aromatic hydrocarbons in the atmosphere: monitoring, sources, sinks and fate. II: sinks and fate. Anal. Chim. 94, 257–268.

Wang, W., Simonich, S.L.M., Wang, W., Giri, B., Zhao, J., Xue, M., Cao, J., Lu, X., Tao, S., 2011. Atmospheric polycyclic aromatic hydrocarbon concentrations and gas/particle partitioning at background, rural village and urban sites in the North China Plain. Atmos. Res. 99, 197–206.

Wang, X., Thai, P.K., Mallet, M., Desservettaz, M., Hawker, D.W., Keywood, M., Miljevic, B., Paton-Walsh, C., Gallen, M., Mueller, J.F., 2017. Emissions of selected semivolatile organic chemicals from forest and savannah fires. Environ. Sci. Technol. 51, 1293–1302.

Wang, Y., 2014. MeteoInfo: GIS software for meteorological data visualization and analysis. Meteorol. Appl. 21, 360–368.

Wang, Y., Zhang, Q., Zhang, Y., Zhao, H., Tan, F., Wu, X., Chen, J., 2019. Source apportionment of polycyclic aromatic hydrocarbons (PAHs) in the air of Dalian, China: correlations with six criteria air pollutants and meteorological conditions. Chemosphere 216, 516–523.

Wei, H., Guangbin, L., Yong, T., Qin, Z., 2015. Emission of polycyclic aromatic hydrocarbons from different types of motor vehicles' exhaust. Environ. Earth Sci. 74, 5557–5564.

Wilson, J.M., Baeza-Romero, M.T., Jones, J.M., Pourkashanian, M., Williams, A., Lea-Langton, A.R., Ross, A.B., Bartle, K.D., 2013. Soot formation from the combustion of biomass pyrolysis products and a hydrocarbon fuel, n-decane: an aerosol time of flight mass spectrometer (ATOFMS) study. Energy Fuel. 27, 1668–1678.

Wu, Z., Lin, T., Li, Z., Jiang, Y., Li, Y., Yao, X., Gao, H., Guo, Z., 2017. Air–sea exchange and gas–particle partitioning of polycyclic aromatic hydrocarbons over the northwestern Pacific Ocean: role of East Asian continental outflow. Environ. Pollut. 230, 444–452.

Yan, D., Wu, S., Zhou, S., Tong, G., Li, F., Wang, Y., Li, B., 2019. Characteristics, sources and health risk assessment of airborne particulate PAHs in Chinese cities: a review. Environ. Pollut. 248, 804–814.

Yang, J., Ma, S., Gao, B., Li, X., Zhang, Y., Cai, J., Li, M., Yao, L.a., Huang, B., Zheng, M., 2017. Single particle mass spectral signatures from vehicle exhaust particles and the source apportionment of on-line PM2.5 by single particle aerosol mass spectrometry. Sci. Total Environ. 593–594, 310–318.

Yang, Y., Guo, P., Zhang, Q., Li, D., Zhao, L., Mu, D., 2010. Seasonal variation, sources and gas/particle partitioning of polycyclic aromatic hydrocarbons in Guangzhou, China. Sci. Total Environ. 408, 2492–2500.

Yao, X., Wang, K., Wang, W., Zhang, T., Wang, W., Yang, X., Qian, F., Li, H., 2020. Reduction of polycyclic aromatic hydrocarbons (PAHs) emission from household coal combustion using ferroferric oxide as a coal burning additive. Chemosphere 252, 126489.

Youping, S., Xin, L., 2015. Source identification, emission characters and tendency of atmospheric PAHs in China: a review. In: Proceedings of the 2015 International Symposium on Material, Energy and Environment Engineering. Atlantis Press, pp. 318–321.

Yu, Y., Katsoyiannis, A., Bohlin-Nizzetto, P., Brorström-Lundén, E., Ma, J., Zhao, Y., Wu, Z., Tych, W., Mindham, D., Sverko, E., Barresi, E., Dryfhout-Clark, H., Fellin, P., Hung, H., 2019. Polycyclic aromatic hydrocarbons not declining in arctic air despite global emission reduction. Environ. Sci. Technol. 53, 2375–2382.

Yuan, Q., Teng, X., Tu, S., Feng, B., Wu, Z., Xiao, H., Cai, Q., Zhang, Y., Lin, Q., Liu, Z., He, M., Ding, X., Li, W., 2020. Atmospheric fine particles in a typical coastal port of Yangtze River Delta. J. Environ. Sci. 98, 62–70.

Zawadowicz, M.A., Froyd, K.D., Murphy, D.M., Cziczo, D.J., 2017. Improved identification of primary biological aerosol particles using single-particle mass spectrometry. Atmos. Chem. Phys. 17, 7193–7212.

Zelenyuk, A., Imre, D., Beránek, J., Abramson, E., Wilson, J., Shrivastava, M., 2012. Synergy between secondary organic aerosols and long-range transport of polycyclic aromatic hydrocarbons. Environ. Sci. Technol. 46, 12459–12466.

Zeng, C., Wang, B., Zhang, H., Sun, M., Huang, L., Gu, Y., Qiu, Z., Müllen, K., Gu, C., Ma, Y., 2021. Electrochemical synthesis, deposition, and doping of polycyclic aromatic hydrocarbon films. J. Am. Chem. Soc. 143, 2682–2687.

Zhan, L., Huang, H., Zhao, S., Wang, Z., Zhang, G., Cheng, H., 2022. Comparison of atmospheric polycyclic aromatic hydrocarbons (PAHs) over six years at a CAWNET background site in central China: changes of seasonal variations and potential sources. Chemosphere 299, 134298.

Zhang, H., Hu, D., Chen, J., Ye, X., Wang, S.X., Hao, J.M., Wang, L., Zhang, R., An, Z., 2011. Particle size distribution and polycyclic aromatic hydrocarbons emissions from agricultural crop residue burning. Environ. Sci. Technol. 45, 5477–5482.

Zhang, J., Liu, L., Xu, L., Lin, Q., Zhao, H., Wang, Z., Guo, S., Hu, M., Liu, D., Shi, Z., Huang, D., Li, W., 2020. Exploring wintertime regional haze in northeast China: role of coal and biomass burning. Atmos. Chem. Phys. 20, 5355–5372.

Zhang, Y., Chen, J., Yang, H., Li, R., Yu, Q., 2017. Seasonal variation and potential source regions of PM2.5-bound PAHs in the megacity Beijing, China: impact of regional transport. Environ. Pollut. 231, 329–338.

Zhang, Y., Pei, C., Zhang, J., Cheng, C., Lian, X., Chen, M., Huang, B., Fu, Z., Zhou, Z., Li, M., 2023. Detection of polycyclic aromatic hydrocarbons (PAHs) using a high performance-single particle aerosol mass spectrometer (HP-SPAMS). J. Environ. Sci. 124, 806–822.

Zhou, S., Lee, A.K.Y., McWhinney, R.D., Abbatt, J.P.D., 2012. Burial effects of organic coatings on the heterogeneous reactivity of particle-borne benzo[a]pyrene (BaP) toward ozone. J. Phys. Chem. A 116, 7050–7056.

Zhou, S., Shiraiwa, M., Mcwhinney, R.D., Pöschl, U., Abbatt, J., 2013. Kinetic limitations in gas-particle reactions arising from slow diffusion in secondary organic aerosol. Faraday Discuss 165, 391–406.

Zhu, F.-J., Arina, S.-Z.-L., Zhang, Z.-F., Liu, L.-Y., Song, W.-W., Cheng, Y., Liu, J.-M., Ma, W.-L., 2022. Non-equilibrium influence on G/P partitioning of PAHs: evidence from the diurnal and nocturnal variation. Chemosphere 294, 133722.